Available online at www.derpharmachemica.com

ISSN 0975-413X
CODEN (USA): PCHHAX

Der Pharma Chemica, 2016, 8(20):78-84
(http://derpharmachemica.com/archive.html)

Microwave assisted synthesis of ZnO and Co doped ZnO nanoparticles and their antibacterial activity

M. Sheik Muhideen Badhusha*

Department of Chemistry, SadakathullahAppa College, Tirunelveli, Tamilnadu, India

---

ABSTRACT

The aim of this study was to obtain and characterize ZnO and Co doped ZnO nanoparticles by Microwave assisted method. ZnO plays an important role in many semiconductors technological aspects. In this work, the Co doped ZnO nanoparticles prepared by varying the concentration of Co $(CH_3COO)_2.4H_2O$. The synthesized nanomaterials were characterized by XRD, FT-IR and SEM with EDX. The XRD patterns showed that ZnO nanoparticles have hexagonal wurtzite structure. The FT-IR study confirms the presence of functional group in ZnO. SEM photographs show that the synthesized pure ZnO and Co doped ZnO were in the shape of nanoneedles and nanospheres. The average size of nanoneedles and nano-spheres were found to be 25-35 nm and 20-30 nm.

Keywords: ZnO, Co-ZnO, Microwave, Antibacterial activity.

INTRODUCTION

Metallic oxide nanoparticles, specifically nano-scale ZnO, have gained considerable importance in recent years due to their wide range of applications in various fields of science notably biotechnology and pharmacology [1]. ZnO nanoparticles have been regarded as biocidal agents/disinfectants because of their safety, lower toxicity and biocompatibility towards humans [2].

Number of synthesis methods are available for the preparation of pure and doped ZnO nanomaterials, like hydrothermal, hydrolysis, sol–gel, vapor condensation, spray pyrolysis and organic precursor flame decomposition [3]. In conventional synthesis, energy is transferred to the material through convection, conduction and radiation, which results in temperature gradient between surface and bulk. The microwave heating causes the uniform distribution of temperature between the surface and the bulk material and thereby leading to the fast formation of nanoparticles. The microwave dielectric heating has resulted in acceleration of the chemical transformations in a microwave field, which cannot be achieved easily by the conventional method [4-5].

Due to the outbreak of the infectious diseases caused by different pathogenic bacteria, the scientists are searching for new antibacterial agents. In the present scenario, nanoscale materials have emerged up as novel antimicrobial agents owing to their high surface area to volume ratio and the unique chemical and physical properties [6]. Nowadays, ZnO is more focussed by researchers due to its stability and antibacterial activity during rough and tough processing and safe materials for human and ecosystem [7]. Antimicrobial activity of ZnO has enhanced due to the presence of water molecules on its surface, these aqueous suspensions of ZnO and water generate free radicals of hydroxyl and oxygen species which is responsible for remarkable oxidative stress in treated bacterial cells. Recently, many complexes and nanomaterials of Co(II) showing antimicrobial [8]. But, there are significant results over antibacterial

activity of cobalt doped ZnO while both zinc and cobalt are the essential elements of human and animal health in trace amounts. Earlier reports have been mainly focused on optical, electrical and magnetic properties of Co doped ZnO NPs [9], whereas very few attempts have been made to study the antibacterial properties of Co doped ZnO NPs. Hence, in the present study, Co doped ZnO nanostructured materials have been successfully synthesized by the microwave assisted method. Further, the influence of Co dopant concentration on the structural, optical, and antibacterial properties of ZnO NPs has been investigated.

MATERIALS AND METHODS

2.1. Chemicals

Zinc acetate dihydrate ($Zn(CH_3COO)_2 \cdot 2H_2O$), cobalt acetate tetrahydrate ($Co(CH_3COO)_2 \cdot 4H_2O$) and Sodium hydroxide (NaOH) were purchased from Merck Private Limited as Analytical grade chemicals.

2.2. Synthesis procedure

Pure and Co doped ZnO with compositional formula $Zn_{1-x}Co_xO$ (x = 0.00, 0.01, 0.03 and 0.05) were synthesized by Microwave assisted hydrothermal route. Appropriate amounts of zinc acetate and cobalt acetate were dissolved in water and stirred using magnetic stirrer for 10 min. 1M solution of NaOH was slowly added into above the mixture solution. Then PEG was added drop by drop into the above solution, which was stirred with a magnetic stirrer, until the pH reached 9.0 and the solution became green. The obtained solution was heated in a LG microwave oven at a power of 300W for 30 min. After microwave processing, the solution was cooled to room temperature. The resulted precipitate was separated by centrifugation, then washed with deionized water and ethanol for several times and finally the precipitate was dried in an oven at 60 °C for 24 h and calcinated at 400 °C for 1 h. ZnO nanoparticles were also prepared by the same procedure without the addition of cobalt acetate.

2.3. Characterization

Structural properties of the synthesized samples were characterized by powder x-ray diffraction (XRD) analysis (X'PERT-PRO diffractometer). Optical properties were analyzed with the help of UV–vis spectrometer (SHIMADZU-UV 1800 spectrometer). Functional group analysis of the synthesized samples was characterized using FT-IR (SHIMADZU- 8400) spectrometer. Morphological properties and composition of the samples were investigated using scanning electron microscopy (SEM, ZEISS Supra 40VP) with energy dispersive x-ray spectroscopy (EDX, Oxford).

2.4. Antibacterial assay

The antibacterial susceptibility test was performed by adopting the agar diffusion method [10]. Around 20 ml of Mueller-Hinton Agar was poured on to the petri plates and allowed to solidify in order to investigate susceptibility test against bacteria. Then 0.1 ml of standardized inoculums suspension was dispensed into the surface of the petri plates and allowed to dry for 5 min. The test solution was prepared with a known weight fraction in 0.01mg/mL of the samples were dissolved in 5% dimethyl sulphoxide (DMSO). Sterile discs (6mm) from Himedia Ltd, Mumbai, were impregnated with 20 µl of the prepared samples (corresponding to 0.05 and 0.1mg / ml) was allowed to dry at room temperature. After drying, the discs with respective samples were placed on the surface of the plate using sterile forceps and gently pressed to ensure contact with the agar surface. The petri dishes were subsequently incubated at 37 ºC for 24 hours. After incubation the growth inhibition rings were quantified by measuring the diameter of the zone of inhibition in mm using transparent ruler in millimeter (including the diameter of the disc) from the lower surface of the petri dishes and the control is consisted of paper disc soaked with appropriate solvent and evaporated to dryness.

RESULTS AND DISCUSSION

3.1 XRD Analysis

Fig. 1 shows the XRD pattern of pure and Co doped ZnO nanoparticles. The peaks that are observed at $2\Theta = 31.70^o$, 34.42^o, 36.19^o, 47.42^o, 56.50^o, 62.66^o and 67.74^o represents the hexagonal wurtzite structure of ZnO with lattice parameters (1 0 0), (0 0 2),(1 0 1), (1 0 2), (1 1 0), (1 0 3) and (1 1 2) (JCPDS card no. 891397). Thus, X-Ray diffraction studies confirmed that the synthesized materials were ZnO and Co doped ZnO with hexagonal phase. Also, all the diffraction peaks agreed with the reported JCPDS data and no characteristic peaks were observed other than ZnO. The average crystallite size is estimated by measuring the change in full-width at the half-maximum of the diffraction peaks using scherrer's formula [11] $D = K\lambda/(\beta\cos\theta)$, where K is the scherrer constant, λ the X-ray

wavelength, β the peak width of half maximum, and θ is the Bragg diffraction angle. The average crystallite size is found to be ~45, ~42, ~21, and ~10 nm correspond to Co concentration (x = 0.00, 0.01, 0.03 and 0.05), respectively. The results of the analysis indicate that the average crystallite size tends to decrease with increasing Co concentrations.

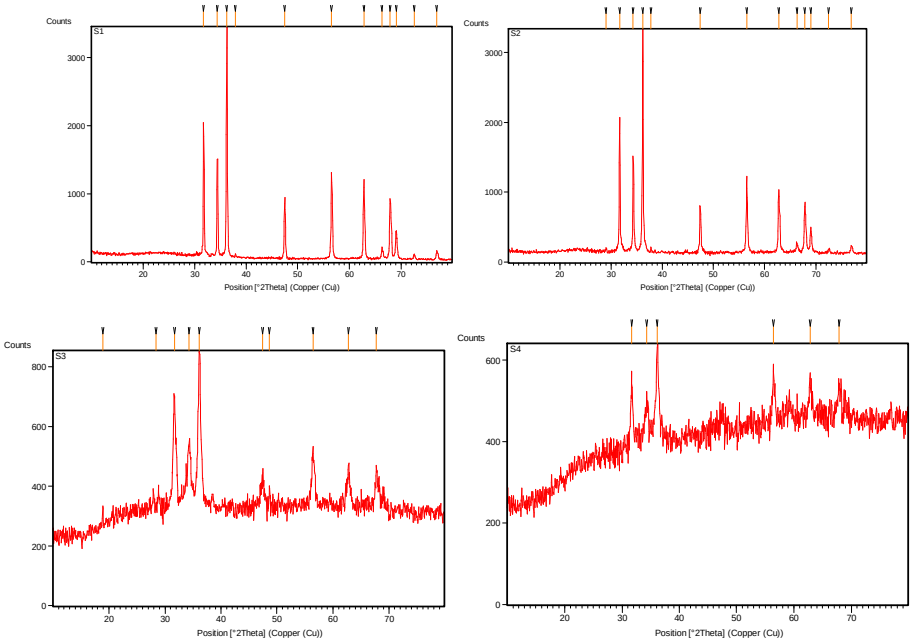

Fig. 1 XRD pattern of pure ZnO and Co doped ZnO NPs

3.2 UV- Vis Analysis

The UV-Vis spectrum of the ZnO and Co doped ZnO nanoparticles were observed by dispersing the powder in deionized water. Fig. 2(a), shows the UV-Vis spectrum of pure ZnO and Co doped ZnO nanoparticles. From the Co doped ZnO shows the higher optical absorption in the visible region than pure ZnO. The fundamental absorption which corresponds to electron excitation from the valence band to conduction band can be used to determine the value of the optical band gap. The value of the optical band gap is calculated by extrapolating the straight line position of $(\alpha h\nu)^2$ vs hν. It is obviously clear that doped ZnO NPs shows reduced the band gap energy than the pure ZnO (Fig. 2b) and it is better than the earlier report. The remarkable changes that, there is a decrease in the band gap for the Co doped ZnO which shows the clear red shift.

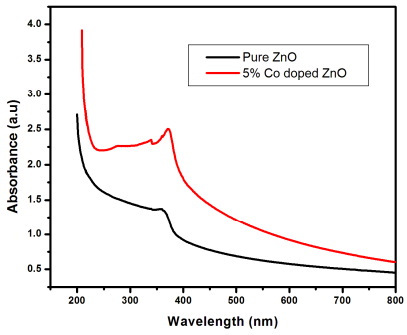

Fig 2 (a) UV–vis absorption spectra of ZnO and Co doped ZnO NPs

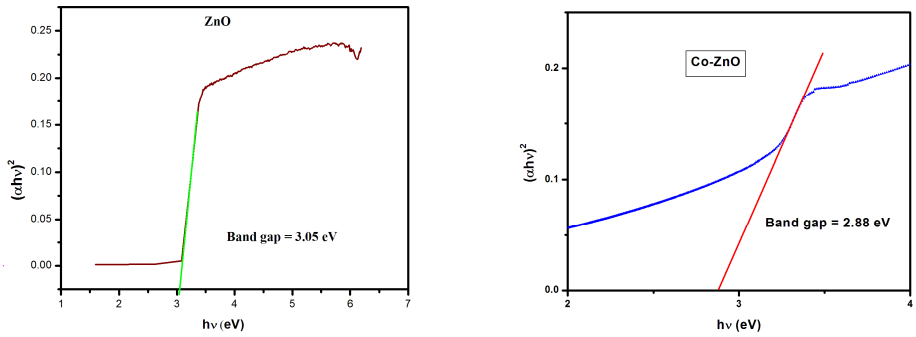

Fig. 2 (b) Tauc plot of $(\alpha h\nu)^2$ versus (hν) of ZnO and Co doped ZnO NPs

3.3 FT-IR Analysis

The FT-IR spectra of ZnO and Co doped ZnO NPs recorded in the range 4000–400 cm^{-1} are shown in Fig. 3. The broad band located around 3450 cm^{-1} is due to O – H stretching vibration of adsorbed water molecules, while the band located about 1625 cm^{-1} is due to O–H bending vibration of the same atmospheric water [12]. The characteristic band at 2350 cm^{-1} is due to O = C = O stretching vibrations of residual CO_2 that is adsorbed on particles surface. The strong absorption band at 444 cm^{-1} is due to Zn–O stretching mode of ZnO nanoparticles [13].

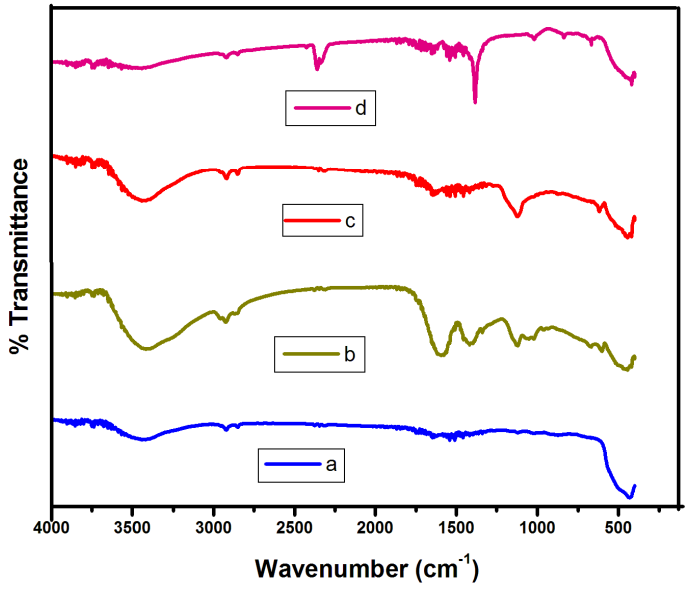

Fig. 3 FT-IR spectrum of ZnO and Co doped ZnO NPs

3.4 SEM Analysis

Surface morphological studies of undoped and Co doped ZnO NPs have been carried out using a scanning electron microscope. Fig. 4 shows representative SEM images for the $Zn_{1-x}Co_xO$ with (x = 0.00, 0.01, 0.03 and 0.05). These images show the presence of large aggregates of smaller individual nanoparticles of various sizes. Pure ZnO showed needle shaped microstructure, while the Co doped ZnO nanoparticles were obtained as nanospheres. For the pure ZnO, the average grain size was found to be around 25-35 nm. The average grain size slightly tends to decrease with increasing the Co doping. This tendency was also observed in the XRD measurements.

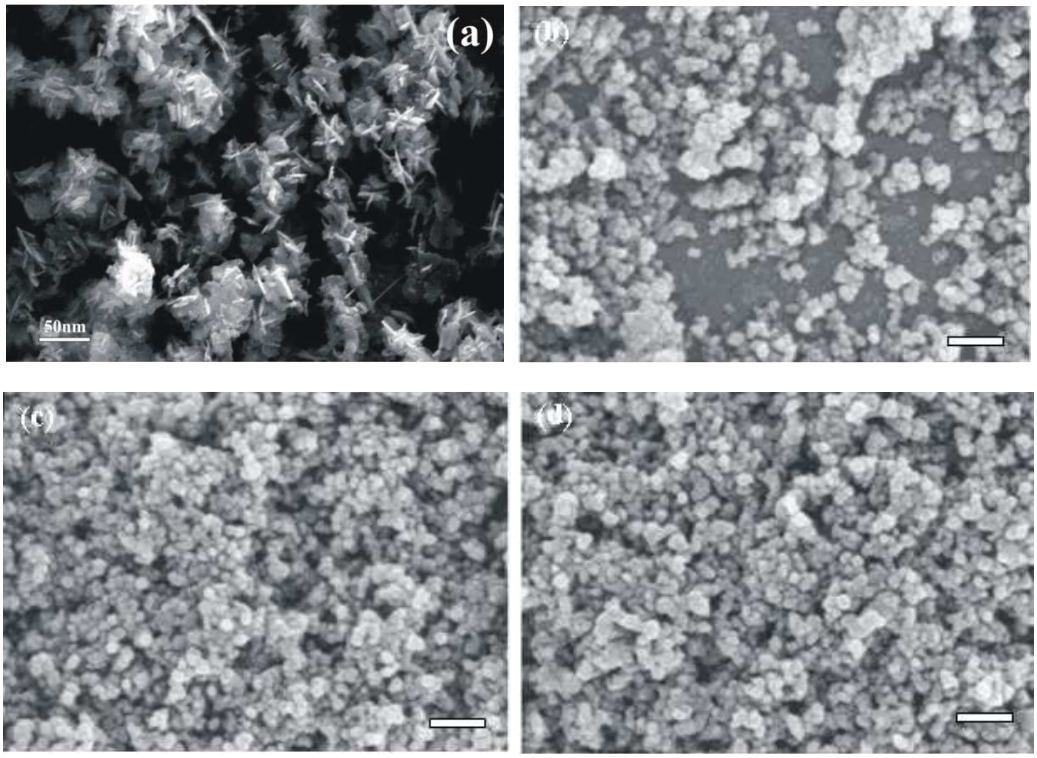

Fig. 4. SEM images for representative samples of $Zn_{1-x}Co_xO$ with (a) x = 0.0, (b) x = 0.01, (c) x = 0.03 and (d) x = 0.05

3.5 Elemental analysis (EDS)

The chemical compositions of synthesized Co doped ZnO NPs were measured by EDS spectra and shown in Fig. 5. The EDS spectrum showed signals of all the expected elements Zn,O and Co, which confirms the presence of Co^{2+} ions which are substituting the Zn^{2+} ions in the Zn matrix. Hence, these results conclude that Co ions have been doped into the ZnO lattice without any impurities.

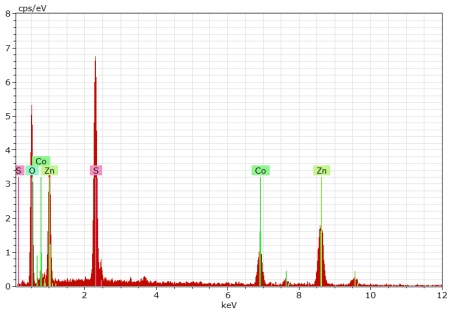

Fig. 5 EDS spectrum of Co doped ZnO NPs

3.6. Antibacterial activity

Antibacterial activity of the synthesized ZnO and Co doped ZnO NPs were evaluated using agar diffusion method. Figs. 6(a)–(f) shows the three different concentrations of bare ZnO and Co doped ZnO NPs suspensions tested against *Salmonella typhi* and *Klebsiella pneumonia*. This indicates the biocidal action of both the samples. For *Salmonella typhi*, bare ZnO NPs exhibited a maximum inhibition zone of 16 mm whereas Co-doped ZnO exhibited inhibition zone of 25 mm. In addition, against *Klebsiella pneumonia* with zone of inhibition of 18 mm is observed for Co-doped ZnO while 14 mm is measured for bare ZnO NPs. It is apparent that, as the concentration of nanoparticles increases the inhibition zone also gets increased. Also, Co-doped ZnO obtained better results in both the bacterial strains.

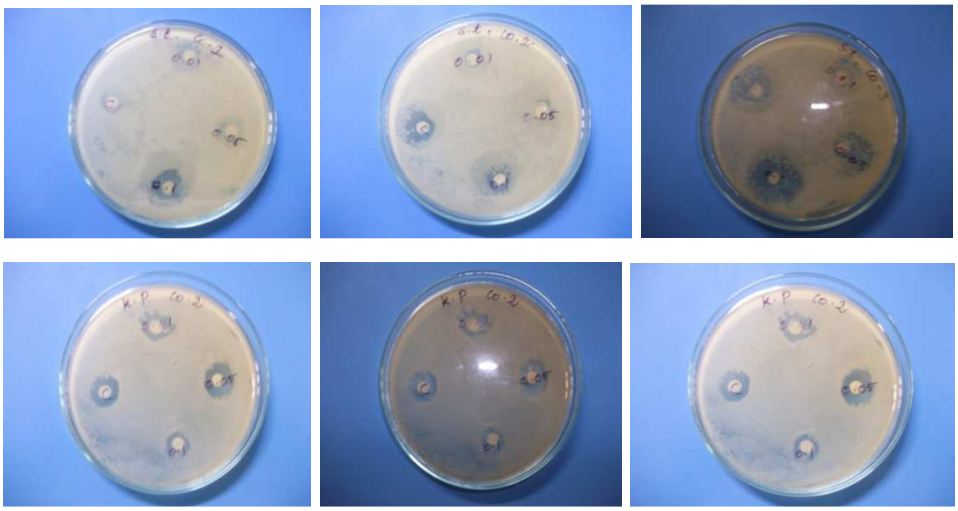

Fig. 6 Antibacterial-screening results against of *Salmonella typhi* and *Klebsiella pneumonia* with Pure ZnO and Co doped ZnO NPs

CONCLUSION

Nanostructured $Zn_{1-x}Co_xO$ (x = 0.00, x = 0.01, x = 0.03 and x = 0.05) nanopowders have been successfully fabricated by microwave-assisted method further analyzed through X-ray diffraction, UV-Visible spectrum, Scanning electron microscopy and Fourier transform infrared spectroscopy to analyzing the influence of Co doping on structural and optical properties of ZnO Nanoparticles. From XRD analysis it is witnessed that average crystalline size decreased with increase of dopant (Co) concentration. SEM images showed the formation of needle like ZnO nanoparticles and in the case of Co doped ZnO nanoparticles are almost spherical images due to the influence of Co doping. The vibration frequencies in the FT-IR spectra further confirm the formation of wurtzite structure. Further, focused on the applied part of synthesized cobalt doped ZnO nanoparticles as an effective and potent antibacterial agent against water borne bacteria. The future studies will probably witness important novel developments in applied nanoresearch regarding antimicrobial agent.

Acknowledgement
I am thankful to the University Grants Commission, Hyderabad, for the financial support provided to me for pursuing the Minor Research Project (Ref. No. F MRP-5363/14 (SERO/UGC)). Also, I express my sincere thanks to the Managing Committee and the Principle, Sadakathullah Appa College, Tirunelveli for having provided to me the necessary facilities to carry out the project successfully.

REFERENCES

[1] R. Javed, M. Usman, S. Tabassum, M. Zia, *Applied Surface Science*., **2016**, 386, 319–326
[2] K.I. Bogutska, Y.P. Sklyarov, Y.I. Prylutskyy, *Ukrainica Bioorganica Acta*., **2013**, 1, 9-16.
[3] I. Djerdj, J. Zvonko, A. Denis, N. Markus, *Nanoscale*., **2010**, 2, 1096–1104.
[4] C. Ragupathi, J. Judith Vijaya, L. John Kennedy, *Materials Science and Engineering B.*, **2014**, 184, 18–25.
[5] Naghmeh Faal Hamedani, Ali Reza Mahjoub, Abbas Ali Khodadadi, Yadollah Mortazavi, *Sensors and Actuators B.*, **2011**, 156, 737– 742.
[6] Razieh Jalal, K. Elaheh, Goharshadia, Maryam Abareshi, Majid Moosavi, Abbas Yousefi, Paul Nancarrow, *Materials Chemistry and Physics*., **2010**, 121, 198–201.
[7] P.K. Stoimenov, R.L. Klinger, G.L. Marchin, K.J. Klabunde, *Langmuir*., **2002,** 18, 679–6686.
[8] Mohammad Oves, Mohd Arshad, Mohd S. Khan, Abraham S. Ahmed, Ameer Azam, Iqbal M.I. Ismail, *Journal of Saudi Chemical Society*., **2015**, 19, 581–588.
[9] H. S. Al-Salman and M. J. Abdullah., *Mater. Sci. Eng. B*, **2013**, 178, 1048–56.
[10] M. Sheik Muhideen Badhusha and C. Joel, *Der Pharmacia Lettre*., **2016**, 8, (11) 218-223.
[11] S. Som and S.K. Sharma, *J. Phys. D: Appl. Phys*., **2012**, 45, 415102.

[12] A. Mesaros, D. Cristina, Ghitulica, M. Popa, R. Mereu, A. Popa, T. Petrisor, S. Vasile, *Ceramic International*., **2014**, 40, 2835–2846.
[13] S. Fabbiyola, L. John Kennedy, Udaya Aruldoss, M. Bououdina, A.A. Dakhel, J. JudithVijaya, *Powder Technology*., **2015**, 286, 757–765.